

---

# Application of the MST clustering to the high energy $\gamma$ -ray sky.

## IV - Blazar candidates found as possible counterparts of photon clusters

R. Campana • E. Massaro • E. Bernieri

**Abstract** We present the results of a cluster search in the *Fermi*-LAT Pass 8  $\gamma$ -ray sky by means of the Minimum Spanning Tree algorithm, at energies higher than 10 GeV and at Galactic latitudes higher than  $25^\circ$ . The selected clusters have a minimum number of photons higher than or equal to 5, a high degree of concentration, and are without a clear corresponding counterpart in blazar catalogues. A sample of 30 possible  $\gamma$ -ray sources was obtained. These objects were verified by applying the standard Maximum Likelihood analysis on the *Fermi*-LAT data. A search for possible radio counterparts in a circle having a radius of  $6'$  was performed, finding several interesting objects, the majority of them without optical spectroscopical data. These can be considered as new blazar candidates. Some of them were already noticed as possible blazars or Active Galactic Nuclei in previous surveys, but never associated with high energy emission. These possible counterparts are reported and their properties are discussed.

**Keywords**  $\gamma$ -rays: observations –  $\gamma$ -rays: source detection

### 1 Introduction

The *Fermi*-Large Area Telescope (LAT) sky survey at  $\gamma$ -ray energies has shown that blazars constitute the

largest class of extragalactic high energy sources (see, e.g., the review paper by Massaro et al. 2016). For this reason, since a few years the searches for new blazars based on multifrequency approaches have been very successful, providing new samples of blazars and candidates as, for example, WIBRaLS (D’Abrusco et al. 2014) and 1WHSP (Arsioli et al. 2015).

Campana et al. (2015, Paper I) applied successfully the Minimum Spanning Tree (hereafter MST) algorithm for searching new spatial clusters of  $\gamma$  rays which could be an indication for localized faint high energy sources. In particular, it was illustrated how MST is useful for finding clusters having a small number of photons, but likely related to pointlike sources.

In two other previous papers (Campana et al. 2016b,a, hereafter Paper II and III) we reported samples of blazars and blazar candidates associated with photon clusters found by means of the MST algorithm. These sources were included in the 5th Edition of the Roma-BZCAT (Massaro et al. 2014) and in the 1WHSP sample.

In this paper we extend our MST analysis of the *Fermi*-LAT  $\gamma$ -ray sky at energies higher than 10 GeV, reporting the discovery of 30 new photon clusters not associated with known blazars but having interesting radio counterparts with blazar-like characteristics at angular distances lower than a few arcminutes. Some of them were already reported in recent samples of quasar candidates. Optical spectra are available from the Sloan Digital Sky Survey (SDSS, Alam et al. 2015) for four objects and only one from the 6dF survey (Jones et al. 2004, 2009), therefore for a better classification we considered the mid-infrared photometric colours from the WISE (Wide-field Infrared Survey Explorer, Wright et al. 2010) database according the criteria introduced by Massaro et al. (2011) and for the WIBRaLS sample D’Abrusco et al. (2012). As in the

---

R. Campana

INAF/IASF-Bologna, Via Gobetti 101, I-40129, Bologna, Italy.

E. Massaro

INAF/IAPS, via del Fosso del Cavaliere 100, I-00133, Roma, Italy

In Unam Sapientiam, Roma, Italy

E. Bernieri

INFN - Sezione di Roma Tre, via della Vasca Navale 84, I-00146 Roma, Italy.

previous papers, in this search we considered the Fermi-LAT Pass 8 sky for Galactic latitudes higher than  $|25^\circ|$ .

## 2 Photon cluster detection by means of the MST algorithm

The Minimum Spanning Tree (Campana et al. 2008, 2013) is a source-detection algorithm useful for searching clusters in a field of points. A brief description of MST was presented elsewhere (e.g. in Paper I), and therefore we provide here only a brief summary of this method.

Consider a two-dimensional set of  $N$  nodes: one can define a set  $\{\lambda_i\}$  of weighted edges connecting them. The MST is the unique tree (i.e. a graph without closed loops) that connects all the nodes with the minimum total weight, defined as  $\min[\sum_i \lambda_i]$ . For a set of points in a Cartesian frame, the edges are the lines joining the nodes and the weights are their lengths, while for a region on the celestial sphere the edge weights are the angular distances between pairs of photons.

Once the MST is computed, a set of subtrees corresponding to clusters of photons is extracted by means of a *primary* selection, consisting of: *i) separation*: remove all the edges having a length  $\lambda > \Lambda_{\text{cut}}$ , the separation value, defined in units of the mean edge length  $\Lambda_m = (\sum_i \lambda_i)/N$ , obtaining a set of disconnected subtrees; *ii) elimination*: remove all the sub-trees having a number of nodes  $n \leq N_{\text{cut}}$ , leaving only the clusters having a size over a fixed threshold. The remaining set of sub-trees provides a first list of candidate cluster and a *secondary* selection is applied to extract the most robust candidates for  $\gamma$ -ray sources. The suitable parameter for this selection (Campana et al. 2013), also useful for evaluating the “goodness” of the accepted clusters, is the *magnitude* of the cluster:

$$M_k = n_k g_k \quad (1)$$

where  $n_k$  is the number of nodes in the cluster  $k$  and the *clustering parameter*  $g_k$  is the ratio between  $\Lambda_m$  and  $\lambda_{m,k}$ , the mean length of the  $k$ -th cluster edges. The probability to obtain a given magnitude value combines that of selecting a cluster with  $n_k$  nodes together with its “clumpiness”, compared to the mean separation in the field. It was found that  $\sqrt{M}$  is a good estimator of statistical significance of MST clusters. In particular, a lower threshold value of  $M$  around 15–20 would reject the large majority of spurious (low significance) clusters.

The cluster centroid coordinates are obtained by means of a weighted mean of the photons’ coordinates (Campana et al. 2013). If the cluster can be associated

with a genuine pointlike  $\gamma$ -ray source, the radius of the circle centred at the centroid and containing the 50% of photons in the cluster, the *median radius*  $R_m$ , should be smaller than or comparable to the 68% containment radius of instrumental Point Spread Function (PSF, see Ackermann et al. 2013).

## 3 The MST cluster populations

As reported in Papers II and III, *Fermi*-LAT data (Pass 8) above 10 GeV, covering the whole sky in the 7 years time range from the start of mission (2008 August 04) up to 2015 August 04, were downloaded from the FSSC archive<sup>1</sup>. Standard cuts on the zenith angle and data quality were applied.

We searched for cluster of  $\gamma$  photons by means of MST in the sky after the exclusion of the Galactic belt up to a latitude  $|b| \leq 25^\circ$  to reduce the possibility of finding clusters originated by local high background fluctuations. Each of these two broad regions was then divided into ten smaller parts where MST was applied. Regions were selected with  $2^\circ$  width overlapping strips along their boundaries to avoid missing clusters; in the case of multiple detections the cluster with the highest  $M$  was inserted in the sample. The parameters of primary selection of clusters were  $N_{\text{cut}} = 4$  and  $\Lambda_{\text{cut}} = 0.7 \Lambda_m$ ; then a secondary selection was applied with  $M > 20$ , that according to the results of Campana et al. (2013) gives a very low probability to select spurious clusters.

A sample of 919 clusters was obtained, of which 716 have a firm 3FGL counterpart. For 165 1FHL counterparts were found, five of which not in the 3FGL catalogue, From the residual sample of 198 clusters we then sorted out 16 clusters that were found associated with 1WHSP sources (Paper II), 35 other clusters very close to blazars in the 5BZCAT catalogue (Papers I and III), 5 corresponding to  $\gamma$ -ray sources in the recent 2FHL catalogue at energies higher than 50 GeV (The Fermi-LAT Collaboration 2015) and 1 corresponding to the GRB 130427A (Maselli et al. 2014; Ackermann et al. 2014). Thus, the final sample contains 141 clusters not related to previously known  $\gamma$ -ray sources or blazars.

From the latter sample, a further subselection was made by applying the following criteria: *i) M > 25*, or *ii) g > 3*. Note that the latter criterium is particularly strong, because it selects clusters with a high photon concentration, as expected from point-like sources, while extended features or close cluster pairs are more efficiently rejected, as already discussed in Campana

<sup>1</sup><http://fermi.gsfc.nasa.gov/ssc/data/access/>

**Table 1** New MST clusters at  $E > 10$  GeV and their possible counterparts. Columns 2–7 report the MST parameters of the MST cluster, column 8 gives the J2000 positions in the AllWISE catalog and in column 9 the angular distance to the cluster centroid is given.

MST cluster	RA J2000	DEC J2000	$n$	$g$	$M$	$R_m$ deg	AllWISE source	$\Delta\theta$ '	Notes
MST 0041–1608	10.433	–16.137	5	7.040	35.198	0.042	J004141.21–160747.2	0.82	
MST 0059–3512	14.856	–35.214	9	3.723	33.511	0.128	J005931.47–351049.1	2.39	
MST 0133–4533	23.339	–45.558	6	7.133	42.800	0.034	J013309.28–453524.0	2.80	
MST 0135+0257	23.790	2.951	5	4.012	20.062	0.074	J013507.04+025542.6	1.53	
MST 0137+2247	24.491	22.793	9	3.635	32.719	0.068	J013801.12+224808.7	0.96	
MST 0201–4348	30.272	–43.800	5	4.052	20.260	0.073	J020110.93–434655.5	1.48	
MST 0207–2403	31.899	–24.054	7	3.578	25.043	0.067	J020733.39–240202.0	1.32	
MST 0310–1039	47.715	–10.657	8	2.872	22.973	0.108	J031034.10–103714.9	4.83	
MST 0338–2850	54.719	–28.841	14	3.389	47.443	0.089	J033859.60–284619.9	4.39	cnf
MST 0350+0640	57.505	6.677	7	4.437	31.062	0.041	J034957.83+064126.2	1.16	cnf
MST 0350–5146	57.605	–51.774	6	6.662	39.970	0.059	J035028.30–514454.3	1.78	cnf
MST 0359–0235	59.872	–2.590	8	3.077	24.613	0.065	J035923.48–023501.8	1.50	
MST 0703+6808	105.830	68.144	5	4.402	22.012	0.048	J070315.90+680831.2	0.34	cnf
MST 0805+3835	121.488	38.589	9	4.201	37.811	0.056	J080551.75+383538.0	1.07	
MST 1020+0510	155.011	5.167	9	2.981	26.833	0.140	J102015.12+050910.6	3.23	cnf rg
MST 1405–1853	211.481	–18.892	8	5.039	40.312	0.033	J140545.58–185123.8	3.15	
MST 1410+1438	212.623	14.643	7	4.747	33.232	0.060	J141028.05+143840.2	0.36	rg
MST 1427–1823	216.859	–18.399	12	4.112	49.347	0.087	J142725.93–182303.7	0.88	cp
MST 1431–3122	217.793	–31.372	15	3.073	46.092	0.076	J143109.22–312038.8	1.71	
MST 1439–2524	219.872	–25.415	7	5.569	38.981	0.041	J143934.65–252459.1	1.22	
MST 1503+1651	225.852	16.862	6	4.588	27.529	0.042	J150316.56+165117.6	1.93	cnf
MST 1514–0949	228.679	–9.830	12	2.764	33.172	0.102	J151449.75–094838.4	2.00	
MST 1546–1002	236.569	–10.034	9	3.191	28.720	0.078	J154611.48–100326.1	1.88	
MST 1547–1531	236.823	–15.521	9	4.584	41.258	0.054	J154725.68–153237.0	2.42	cp SD
MST 1605–1142	241.262	–11.706	9	3.882	34.936	0.060	J160517.53–113926.8	4.62	
MST 1640+0640	250.044	6.478	6	3.586	21.518	0.025	J164011.05+062826.9	0.25	
MST 1643+3317	250.943	33.293	10	3.054	30.540	0.055	J164339.46+331647.8	1.62	cnf
MST 1716+2307	259.034	23.129	7	5.267	36.871	0.027	J171603.22+230822.9	1.31	
MST 2037–3836	309.436	–38.607	5	4.192	20.958	0.061	J203733.38–383635.8	2.19	
MST 2245–1734	341.389	–17.575	6	3.405	20.432	0.044	J224531.85–173358.9	0.64	

Notes:

cnf: possible counterpart confusion;

rg: possible radio galaxy;

cp: close pair;

SD; coordinates from SDSS.

et al. (2016a). It should be noticed that, however, sources with  $g \leq 3$  have been shown to be sometimes significant. Then, the ASDC sky explorer tool<sup>2</sup> was used to search within a region of a radius of  $6'$ , that in Campana et al. (2015) has been shown to be optimal for cross-matching, for radio sources from a large set of catalogues, including NVSS (Condon et al. 1998), FIRST (White et al. 1997), SUMSS 2.1 (Mauch et al. 2003), PMN (Gregory et al. 1994), and many others. We considered only sources with possible radio and optical counterparts and obtained a final list of 30 objects which could be considered for a deeper analysis to assess their likely status as blazar candidates. The optical counterparts of the radio sources have been searched using several databases accessible from the ASDC explorer tool, connected to *Vizier* and thus including SDSS, USNO and COSMOS catalogues, and considering the uncertainty on the radio source location. All these sources had also a clear infrared counterpart in the AllWISE (Cutri et al. 2013) catalogue and the positional correspondence was verified in the images<sup>3</sup>. Table 1 reports the main MST parameters of these clusters and the coordinates of the corresponding possible counterparts in the AllWISE catalogue after the accurate verification in multiband IR images. When within the region of interest of some clusters more than one radio source was found, and when the selection of the best radio counterpart (also using literature data) was not safe, the note ‘cnf’ (possible confusion) is added.

Several sources were already reported as blazar candidates in WIBRaLS (D’Abrusco et al. 2014, marked as WBR in the following Table 2) or as QSO by Brescia et al. (2015, B15 in Table 2), or their flat radio spectrum was confirmed by low frequency data Mas-saro et al. (2014, M14 in Table 2); one is in the 1WHSP sample (1WH in Table 2), but not reported in Paper II because the cluster has 5 photons, lower than the minimum number considered in that paper. Only for one source we found a possible correspondence with a high energy source reported in the 3EG catalogue (Hartman et al. 1999), but up to now undetected in the Fermi sky.

#### 4 $TS$ evaluation from ML analysis

We performed also a standard unbinned likelihood analysis for each MST cluster. A Region of Interest (ROI) of  $10^\circ$  radius was selected around the MST cluster centroid, and standard screening criteria were applied to

the *Fermi*-LAT data above 3 GeV. The likelihood analysis was performed considering all the 3FGL sources within  $20^\circ$  from the cluster centroid, as well as the Galactic and extragalactic diffuse emission. A further source with a power-law spectral distribution was assumed at the MST coordinates. The normalization and spectral index of all the 3FGL sources within the ROI was allowed to vary in the fitting, while the parameters of the sources between  $10^\circ$  and  $20^\circ$  from the center of the field of view were fixed to their catalogue values. From this analysis, we derived the likelihood Test Statistics ( $TS$ ) and fluxes in the two 3–300 GeV and 10–300 GeV bands. These results are reported in Table 2 together with some other photometric and spectroscopic data, when available.

We found only five sources with  $\sqrt{TS} < 5$ , but one (MST 0041–1608) is almost borderline ( $\sqrt{TS} = 4.96$ ) and could be considered confirmed. Two of the remaining four clusters, MST 0310–1039 and MST 2245–1734, have  $\sqrt{TS} > 4.5$ , that correspond to a detection significance above roughly  $4.5\sigma$ , therefore can be reasonably considered as safe (although lower than the conventional  $5\sigma$  threshold to be included in the FGL source catalogs), whereas the other two (MST 0201–4348 and MST 2037–3836), with ML significances of 3.5 and 2.3, respectively, are questionable and their actual detection will be discussed in detail the following section.

#### 5 Properties of new blazar candidates

In Table 2 we reported in addition to ML significance and spectral data some other parameters of interest: the radio flux density at 1.4 GHz from NVSS or FIRST, optical magnitude in the  $F$  (photographic red band magnitude  $R$  from The Guide Star Catalog, Version 2.3.2 (GSC2.3, STScI, 2006), or  $r$  (from SDSS) bands and spectroscopic information or the redshift  $z$ , useful for the understanding of the main properties of these blazar candidates.

As apparent in Table 1 all sources have likely AllWISE counterparts and for 25 of them photometric data are given in the  $W1$  ( $13.4 \mu\text{m}$ ),  $W2$  ( $4.6 \mu\text{m}$ ) and  $W3$  ( $12 \mu\text{m}$ ) bandpasses (Table 3). Further 13 of them are also detected in the  $W4$  ( $22 \mu\text{m}$ ) filter. Mas-saro et al. (2013) investigated the nature of unidentified 2FGL sources in the two WISE colour plot by means of the Kernel Density Estimator replacing the constraint on the detection at  $22 \mu\text{m}$  with the occurrence of an associated radio emission. Considering that our candidates are all detected in the radio band, we computed their two WISE colour plot that is shown

<sup>2</sup><http://www.asdc.asi.it/>

<sup>3</sup><http://irsa.ipac.caltech.edu/applications/wise/>

in Figure 1. No reddening correction was applied because at the Galactic latitudes of our sources its largest effect on the colours was of only a few hundredths of magnitude, lower than typical uncertainties. In this plane  $\gamma$ -ray blazars are essentially concentrated within the two coloured areas, defined in the figures reported in Massaro et al. (2013), D’Abrusco et al. (2014), and Massaro and D’Abrusco (2016): BL Lac objects are mainly concentrated in the blue area, while FSRQ are mostly found in the red one. In their data there is no definite boundary between BL Lac and FSRQ regions, and the given separation is only indicative. All our candidates have colours matching very well this *locus*, with a clear dominance for the BL Lac region; there is only one source (MST 1439–2524) just outside the region, but its distance from the boundary is within  $1\sigma$ , not large enough to be significant. Note, in particular, the very close similarity between our plot and that given in Figure 2 of Massaro et al. (2013).

For what concerns the 13 sources with also  $W4$  data, 5 of them, typically those with the highest signal to noise ratio, were also reported in WIBRaLS (Table 2) and therefore are located in the blazar locus in the 3 colour plot (D’Abrusco et al. 2014). Three other sources lie also in the same region, whereas all the remaining 5 have uncertainties on  $W4$  of  $\approx 0.4$  mag and are compatible with the expected position within one standard deviation.

In the following we discuss the individual properties of the candidates.

## 5.1 Comments to individual selected counterparts to MST clusters

### 5.1.1 MST 0041–1608

This cluster with a borderline ML significance has only a possible radio counterpart corresponding to a rather faint object for which few IR and optical photometric data are available. The colours are not in conflict with a possible blazar nature of this object.

### 5.1.2 MST 0059–3512

In the searching circle of this cluster there are four radio sources: the selected one is the brightest, whereas the other fainter radio sources do not have optical counterparts. It is reported in the RASS-6dFGS catalogue of X-ray selected AGN from the 6dF Galaxy Survey by Mahony et al. (2010) with a featureless spectrum characterized by a large blue excess. There is therefore evidence for considering it a HBL (High energy peaked BL Lac, Padovani and Giommi 1995) object.

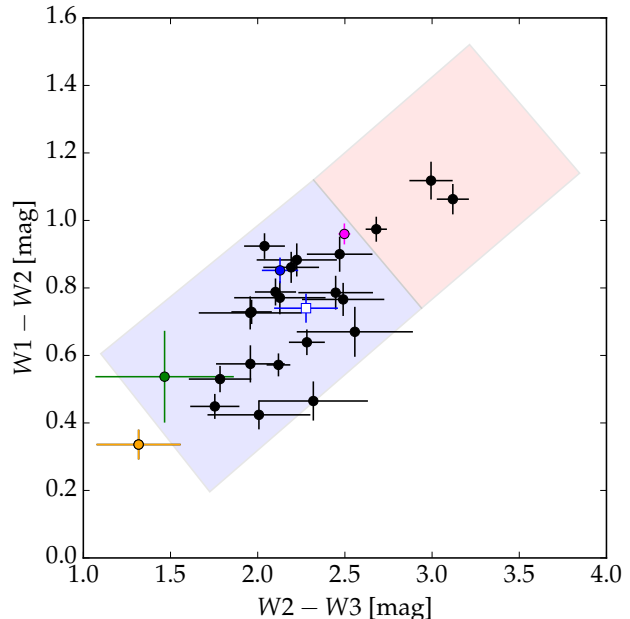


**Fig. 1** Plot of the infrared colours of the MST-selected BL Lac objects from the AllWISE catalogue. The shaded regions define the WISE Blazar locus where are present  $\gamma$ -ray loud blazars. The blue-shaded region represents the locus where there is a concentration of BL Lac objects, while the red-shaded region correspond to FSRQ objects. The green point corresponds to the second counterpart of MST 0350+0640; the magenta point to the counterpart of MST 1431–3122 and the orange point, just outside the blazar region, is that of MST 1439–2524. The blue circle and the open blue square indicate the colours of the WISE candidate counterparts to MST 1546–1002 and MST 1547–1531, respectively, as explained in the text.

### 5.1.3 MST 0133–4533

Two very close optical galaxy-like objects of similar brightness correspond to the SUMSS radio source that has a bright counterpart in the RASS (Voges et al. 1999). In the WISE two-colour plot it is close to the central line of the strip. This source is also reported by Mahony et al. (2010) and in 6dF, but its spectrum is not available. There is a strong possibility that one of the two objects could be a BL Lac, but a further spectroscopic investigation will be useful to confirm its nature.

### 5.1.4 MST 0135+0257

This object of galaxy type in SDSS was reported as the counterpart of the X rays source 1RXS J013506.7+025558 by Mickaelian et al. (2006) and was indicated as QSO candidate by Brescia et al. (2015). No optical spectral data are available.

**Table 2** Standard unbinned likelihood analysis of the *Fermi*-LAT data, see Sect. 4 for details. The columns 3–4 report photon fluxes in units of  $10^{-11}$  ph cm $^{-2}$  s $^{-1}$ . For sources below the usual significance threshold ( $\sqrt{TS} = 5$ ) only upper limits are given. Radio flux densities at 1.4 or 0.8 GHz, optical magnitude, RASS X-ray fluxes (0.1–2.4 keV) in erg cm $^{-2}$  s $^{-1}$  and the redshift, when available, are given in the columns from 6 to 9.

MST cluster	$\sqrt{TS}$	Flux 3–300 GeV	Flux 10–300 GeV	Photon index	$F_{1.4/0.8}$ mJy	$F/r$ mag	$F_X$ $\times 10^{-12}$	z	Notes
MST 0041–1608	5.0	$3.4 \pm 1.5$	$1.3 \pm 0.7$	$1.7 \pm 0.4$	18	18.8	—	—	
MST 0059–3512	7.0	$7.8 \pm 2.2$	$2.0 \pm 0.9$	$2.1 \pm 0.3$	79	18.0	1.93	—	6dF
MST 0133–4533	5.4	$4.7 \pm 1.7$	$1.4 \pm 0.7$	$2.0 \pm 0.4$	16	19.5	2.56	—	s
MST 0135+0257	5.3	$4.5 \pm 1.8$	$2.4 \pm 1.2$	$1.4 \pm 0.9$	22	19.0	0.38	—	r gal B15
MST 0137+2247	7.9	$11.0 \pm 2.7$	$3.3 \pm 1.2$	$2.0 \pm 0.3$	42	18.7	—	—	r WBR B15
MST 0201–4348 *	3.5	< 3.1	< 0.3	—	45	19.8	1.53	—	s XM 1WH
MST 0207–2403	6.4	$7.3 \pm 2.2$	$2.3 \pm 1.0$	$1.9 \pm 0.3$	186	19.5	—	—	WBR
MST 0310–1039	4.5	< 6.2	< 1.3	—	80	18.1	—	—	
MST 0338–2850	8.0	$7.0 \pm 2.4$	$2.8 \pm 1.0$	$1.7 \pm 0.2$	42	17.3	—	—	
MST 0350+0640	6.7	$5.6 \pm 1.8$	$3.1 \pm 1.2$	$1.4 \pm 0.7$	9	—	—	—	(a)
	—	—	—	—	17	17.4	1.48	—	(b)
	—	—	—	—	158	19.9	—	—	(c)
MST 0350–5146	5.8	$5.6 \pm 2.0$	$2.3 \pm 1.0$	$1.7 \pm 0.3$	11	17.5	9.11	—	s
MST 0359–0235	5.8	$7.3 \pm 2.3$	$3.0 \pm 1.2$	$1.7 \pm 0.3$	14	18.6	—	—	
MST 0703+6808	5.1	$3.8 \pm 2.4$	$1.9 \pm 1.1$	$1.5 \pm 1.0$	30	17.6	—	—	M14
MST 0805+3835	7.1	$7.9 \pm 2.1$	$1.8 \pm 0.8$	$2.2 \pm 0.3$	13	20.4	—	nl	r SD WBR
MST 1020+0510	6.3	$9.0 \pm 2.4$	$2.0 \pm 1.0$	$2.2 \pm 0.4$	9	19.9	—	nl	r (d)
	—	—	—	—	2	21.4	—	—	r (e)
	—	—	—	—	10	18.1	—	0.276	r gal SD (f)
MST 1405–1853	5.7	$5.4 \pm 2.0$	$2.1 \pm 1.2$	$1.8 \pm 0.3$	29	18.6	—	—	
MST 1410+1438	8.1	$10. \pm 2.4$	$2.7 \pm 1.0$	$2.1 \pm 0.3$	434	16.7	—	0.144	r SD el WBR
MST 1427–1823	7.4	$11. \pm 2.7$	$2.8 \pm 1.0$	$2.1 \pm 0.3$	48	18.1	—	—	
MST 1431–3122	7.9	$12. \pm 2.8$	$3.1 \pm 1.2$	$2.1 \pm 0.3$	254	18.1	0.27	—	CRT WBR
MST 1439–2524	6.7	$8.3 \pm 2.4$	$2.6 \pm 1.1$	$1.9 \pm 0.4$	35	16.3	—	—	
MST 1503+1651	5.5	$4.2 \pm 1.9$	$1.7 \pm 0.8$	$1.7 \pm 0.4$	13	18.8	—	nl	r SD
MST 1514–0949	10.4	$26. \pm 4.3$	$3.3 \pm 1.2$	$2.7 \pm 0.3$	349	19.1	—	—	CRT
MST 1546–1002	6.4	$10. \pm 2.4$	$2.7 \pm 1.1$	$2.1 \pm 0.3$	52	—	—	—	CRT M14
MST 1547–1531	5.4	$7.3 \pm 2.5$	$2.2 \pm 1.0$	$2.0 \pm 0.4$	10	—	—	—	
MST 1605–1142	5.9	$8.0 \pm 2.6$	$3.0 \pm 1.1$	$1.8 \pm 0.3$	258	17.0	0.28	—	3EG CGR WBR M14
MST 1640+0640	5.5	$5.4 \pm 2.2$	$1.7 \pm 0.8$	$1.9 \pm 0.4$	40	18.3	—	—	
MST 1643+3317	6.3	$5.0 \pm 1.5$	$2.2 \pm 0.8$	$1.6 \pm 0.1$	66	19.9	0.48	—	r gal B15
MST 1716+2307	9.7	$13. \pm 2.6$	$3.0 \pm 1.0$	$2.2 \pm 0.2$	6	19.0	—	—	B15
MST 2037–3836 *	2.3	< 2.7	< 0.3	—	25	19.1	—	—	
MST 2245–1734	4.7	< 5.6	< 0.4	—	41	19.3	—	—	B15

Notes:

\* : poorly significant cluster; (a), (b), (c): see Section 5.1.10; (d), (e), (f): see Section 5.1.15; 6dF: spectrum in 6dF survey; SD: spectrum in SDSS; s: radio flux density from SUMSS at 0.8 MHz; r: r magnitude from SDSS; gal: classified as galaxy in SDSS; nl: no clear emission lines in the spectrum; B15: QSO candidate for Brescia et al. (2015); CRT: CRATES flat spectrum radio source; CGR: CGRaBS source; 3EG: possible correspondence with a 3EG source; WBR: blazar candidate in WIBRaLS (D’Abrusco et al. 2014); M14: LORCAT radio source Massaro et al. (2014); 1WH: blazar candidate in the 1WHSP sample; XM: X-ray flux from XMM database.

### 5.1.5 MST 0137+2247

The proposed counterpart is a flat spectrum radio source and blue starlike object in SDSS, classified as C class BL Lac object candidate by D’Abrusco et al. (2014) and candidate QSO by Brescia et al. (2015).

### 5.1.6 MST 0201–4348

This source is listed as blazar candidate in the 1WHSP catalogue and it is detected in the radio, IR and X-ray bands. The lack of optical spectroscopy does not allow a clear classification.

ML analysis gives a significance for this cluster lower than the acceptance threshold and therefore we extended the MST analysis to the low energy ranges. It resulted that the cluster is found only above 10 GeV: a search at energies higher than 7 GeV gave a cluster at the same position, again with 5 photons but with a lower  $M$  value because of the shorter mean distance

between photons; the same result was obtained at energies higher than 3 GeV, and no cluster resulted in the range 3–7 GeV. We can conclude that, considering its  $M$  value just above the threshold, it is possible that this cluster could be originated by a density fluctuation of the high energy background. However, the possibility that its emission can be detected only in this range cannot in principle be excluded.

### 5.1.7 MST 0207–2403

This flat spectrum radio source is in the CRATES and in the WIBRaLS catalogues. An optical spectrum by Titov et al. (2013) has a too low S/N ratio for a safe classification.

### 5.1.8 MST 0310–1039

Marginal flat spectrum radio source ( $\alpha_r \approx -0.4$ ) with an optical counterpart without spectral data. The

**Table 3** Infrared colours of the likely counterparts from the AllWISE photometric database. See Sections 5.1.10 and 5.1.15 for discussion about sources (b), (d), (e) and (f).

MST cluster	AllWISE counterpart	$W1 - W2$	$W2 - W3$	Notes
MST 0041–1608	J004141.21–160747.2	$0.416 \pm 0.055$	–	
MST 0059–3512	J005931.47–351049.1	$0.424 \pm 0.043$	$2.007 \pm 0.295$	
MST 0133–4533	J013309.28–453524.0	$0.766 \pm 0.049$	$2.490 \pm 0.236$	
MST 0135+0257	J013507.04+025542.6	$0.364 \pm 0.060$	–	
MST 0137+2247	J013801.12+224808.7	$0.729 \pm 0.036$	$1.965 \pm 0.116$	
MST 0201–4348	J020110.93–434655.5	$0.465 \pm 0.058$	$2.319 \pm 0.313$	
MST 0207–2403	J020733.39–240202.0	$0.974 \pm 0.037$	$2.680 \pm 0.061$	
MST 0310–1039	J031034.10–103714.9	$0.575 \pm 0.044$	$1.958 \pm 0.197$	
MST 0338–2850	J033859.60–284619.9	$0.449 \pm 0.037$	$1.754 \pm 0.141$	
MST 0350+0640	J034957.83+064126.2	$0.537 \pm 0.136$	$1.466 \pm 0.397$	(b)
MST 0350–5146	J035028.30–514454.3	$0.639 \pm 0.038$	$2.282 \pm 0.103$	
MST 0359–0235	J035923.48–023501.8	$0.670 \pm 0.074$	$2.557 \pm 0.333$	
MST 0703+6808	J070315.90+680831.2	$0.530 \pm 0.039$	$1.784 \pm 0.179$	
MST 0805+3835	J080551.75+383538.0	$0.924 \pm 0.038$	$2.039 \pm 0.117$	
MST 1020+0510	J101948.28+051328.9	$0.883 \pm 0.049$	$2.224 \pm 0.230$	(d)
MST 1020+0510	J102011.75+050635.5	$0.344 \pm 0.111$	–	(e)
MST 1020+0510	J102015.12+050910.6	$0.234 \pm 0.073$	–	(f)
MST 1405–1853	J140545.58–185123.8	$0.861 \pm 0.046$	$2.192 \pm 0.160$	
MST 1410+1438	J141028.05+143840.2	$0.572 \pm 0.034$	$2.119 \pm 0.068$	
MST 1427–1823	J142725.93–182303.7	$0.788 \pm 0.040$	$2.102 \pm 0.118$	
MST 1431–3122	J143109.22–312038.8	$0.960 \pm 0.031$	$2.497 \pm 0.034$	
MST 1439–2524	J143934.65–252459.1	$0.336 \pm 0.044$	$1.317 \pm 0.241$	
MST 1503+1651	J150316.56+165117.6	$0.786 \pm 0.050$	$2.447 \pm 0.214$	
MST 1514–0949	J151449.75–094838.4	$1.118 \pm 0.056$	$2.994 \pm 0.124$	
MST 1546–1002	J154611.48–100326.1	$0.852 \pm 0.038$	$2.128 \pm 0.104$	
MST 1547–1531	J154725.68–153237.0	$0.740 \pm 0.043$	$2.277 \pm 0.183$	
MST 1605–1142	J160517.53–113926.8	$1.063 \pm 0.045$	$3.119 \pm 0.092$	
MST 1640+0640	J164011.05+062826.9	$0.726 \pm 0.049$	$1.957 \pm 0.295$	
MST 1643+3317	J164339.46+331647.8	$0.444 \pm 0.048$	–	
MST 1716+2307	J171603.22+230822.9	$0.900 \pm 0.052$	$2.470 \pm 0.188$	
MST 2037–3836	J203733.38–383635.8	$0.148 \pm 0.056$	–	
MST 2245–1734	J224531.85–173358.9	$0.771 \pm 0.049$	$2.127 \pm 0.262$	

WISE colours are close to the central line of the blazar region in Figure 1.

#### 5.1.9 MST 0338–2850

There are four radio sources in the interesting field: two without optical counterparts, and another corresponding to a very faint object. More interesting appears the brightest radio source with a safe relatively bright optical counterpart and likely associated with the 2RXP J033900.0–284621 source (Flesch 2010) for which no X-ray flux was found in the data archives. It presents an extended galaxy image and a very close fainter source not well resolved in the WISE images, but the colours

place it close to the midline of the blazar area. No spectral data are available for a good classification.

#### 5.1.10 MST 0350+0640

There are three radio sources within a  $2'$  distance to cluster centroid and therefore the possibility of counterpart confusion cannot be excluded. All these three sources are reported in Table 2. The radio source NVSS J035006+064209 (note *a* in Table 2) does not have an optical counterpart in POSS; there is a very faint source in AllWISE at an angular distance of  $9'6$  from the radio position. The other source, NVSS J034957+064126 (note *b* in Table 2) has a clear optical-IR counterpart and was reported as a QSO or a BL Lac object be-

cause of the nearby presence of the RASS source RX J0350.0+0640, reported as a photometrically variable with a featureless continuum source (Appenzeller et al. 1998) and therefore classified as a BL Lac object. It is also close to the galaxy cluster A0465. The XRT image confirms the presence of the very close source 1SXPS J034957.6+064126 (1st Swift-XRT Point Source catalogue, Evans et al. 2014). Its WISE colours place it in the blazar region (see green point in Figure 1). The third and brightest source, NVSS J035006+064107 (PMN J0350+0641, ATZ A073 in NED, note *c* in Table 2) has a steep radio spectrum ( $\alpha_r \approx -0.7$ ). No optical counterpart is detectable in POSS. NED reports the same note by Appenzeller et al. (1998) despite the radio to X-ray angular distance is about  $1'$  and no X-ray source is detected at its coordinates in the XRT image. The second source appears therefore to be the most likely counterpart.

#### 5.1.11 *MST 0350–5146*

There are three SUMSS sources in the search region, of which only the closest one to the cluster centroid has optical-IR counterpart. This object was also reported by Mahony et al. (2010) in their RASS-6dFGS catalogue of X-ray selected AGN, but no spectroscopic data are available. It has a remarkably flat X-ray spectrum with an energy spectral index close to  $\approx -0.25$ . This object was already reported as a possible BL Lac object in the early ROSAT associations (e.g. Schwoppe et al. 2000) but never confirmed by optical spectroscopy. The detection of a  $\gamma$ -ray counterpart suggests it as an HBL object.

#### 5.1.12 *MST 0359–0235*

The only available data on this radio source are from optical and IR photometric catalogues and its possible blazar nature is indicated by WISE colours; optical spectroscopic data are necessary to support this identification.

#### 5.1.13 *MST 0703+6808*

There are only photometric data from optical and IR surveys, the former ones suggesting a possible galaxy dominance, but in the WISE colour plot it is close to the midline of the BL Lac region. The radio source is reported in the LORCAT catalogue (Massaro et al. 2014) because its low-frequency radio spectral index is 0.21. There are two other fainter NVSS radio sources within a radius of  $\sim 4'$  that could be associated with galaxies. More data are necessary for a safe classification.

#### 5.1.14 *MST 0805+3835*

This source was already indicated as QSO by D’Abrusco et al. (2009) and as a C class  $\gamma$ -ray candidate in WIRaLS (D’Abrusco et al. 2014) SDSS photometry  $r = 20.38$  mag is fainter than the  $RF$  value from the IGLS3 (Smart and Nicastro 2013) by about 1.7 mag (Table 2), suggesting that this object can be highly variable. Two featureless spectra in SDSS database support its classification as a BL Lac object.

#### 5.1.15 *MST 1020+0510*

There are several FIRST radio sources in the searching region of this cluster, but only three of them (whose data are reported in Table 2) have rather safe optical counterparts whereas none of them corresponds to known X-ray sources. The source SDSS J101948.24+051328.8 (note *d* in Table 2) has the flux density of 9.5 mJy in FIRST and a featureless SDSS spectrum but a rather high colour index  $u - r = 1.7$ . Its WISE colours are uncertain because of a possible confusion with a close starlike object, but lie quite well within the BL Lac region. It appears in the QSO candidate lists by D’Abrusco et al. (2009) and Brescia et al. (2015). The possible optical counterpart SDSS J102011.76+050636.1 (note *e* in Table 2) of the this FIRST radio source (the offset in the position is  $\approx 3''$ ) is a starlike object with a large  $u - r = 2.9$ , without any indication of a blazar appearance. The source SDSS J102015.12+050910.5 (note *f* in Table 2) has a radio flux density of 10 mJy and corresponds to a rather faint and red galaxy with a large Ca H&K break and a well apparent broad  $H\alpha$  line. WISE photometry of the latter two sources gives only upper limits in the  $W3$  band. The association of the  $\gamma$ -ray emission to one of these three objects remains quite unsafe.

#### 5.1.16 *MST 1405–1853*

There is only a NVSS radio source inside the searching radius of  $6'$ . It has a point-like optical counterpart having all the three WISE colours ( $W1 - W2 = 0.86 \pm 0.05$ ,  $W2 - W3 = 2.19 \pm 0.16$ ,  $W3 - W4 = 2.37 \pm 0.44$ ) compatible with a BL Lac classification according to the WRIBRaLS criteria (D’Abrusco et al. 2014). It appears, therefore, to be a quite good candidate for an HBL object.

#### 5.1.17 *MST 1410+1438*

Very close to the cluster centroid there is a compact radio source with the highest flux density in our sample and a borderline  $[1.4-4.85]$  GHz spectral index close



to  $-0.5$ , but flatter at lower frequencies. The optical counterpart is one of a couple of galaxies at the same  $z = 0.144$  and at an angular distance of  $\approx 30''$  (see Figure 2, left panel). It has a low Ca H&K break ratio ( $\approx 0.15$ ), an emission H $\alpha$  line and the SDSS  $r$  is equal to 16.7 mag. It is reported as a C class  $\gamma$ -ray BL Lac object candidate in WIBRaLS. According to the 5BZCAT criteria it could be classified as a galaxy-dominated blazar.

#### 5.1.18 MST 1427–1823

The optical counterpart to the unique radio source in the field is a point-like object with WISE colours suggesting a blazar candidate (see Figure 2, central panel). Optical spectroscopy is necessary to confirm this classification.

#### 5.1.19 MST 1431–3122

It is the cluster with the highest photon number in the sample. The PKS and CRATES radio source here indicated as possible counterpart was proposed as B class BL Lac and  $\gamma$ -ray source candidate in WIBRaLS. It is also detected in the RASS. The 6dF spectrum is apparently featureless with a possible emission line at the blue end that, if due to CIV, would imply a redshift  $z = 1.632$ . At an angular distance of  $1'.6$  there is also a SUMSS21 source with a flux density of 25 mJy, a very faint optical counterpart and a corresponding WISE source.

#### 5.1.20 MST 1439–2524

The optical counterpart to the NVSS source is at a few arcseconds from a brighter star and the only available data are photometry from general surveys. The WISE colours are close to the blazar area and particularly  $W2 - W3$  is the lowest in all the sample not far from the region of galaxies (orange point in Figure 1). These poor data does not allow to safely establish its nature and whether it is or not the counterpart to the  $\gamma$ -ray cluster and the possibility of a chance association cannot be excluded.

#### 5.1.21 MST 1503+1651

Six radio sources are within the searching circle of this cluster, and only the selected one has an optical counterpart. WISE colours ( $W1 - W2 = 0.79 \pm 0.05$ ,  $W2 - W3 = 2.45 \pm 0.21$ ) locate this object near the centre of the blazar region. It is in the list of QSO candidates in WIBRaLS, while the SDSS spectrum with a featureless blue continuum strongly supports the HBL classification.

#### 5.1.22 MST 1514–0949

There are some peculiarities on this cluster: it has the lowest  $g$  values in the sample but it is curiously associated with the highest  $\sqrt{TS}$ . An analysis with  $\Lambda_{\text{cut}} = 0.6 \Lambda_m$  found again a significant cluster of 8 photons with  $g = 3.508$  at the same coordinates. It should be considered that this cluster is close to the bright source 3FGL J1512.8–0906 ( $\Delta\theta = 0^\circ.86$ ), associated with the FSRQ PKS 1510-08 (Abdo et al. 2010c), well found in our analysis with  $n = 278$  and  $M = 1997$ , and even closer to 3FGL J1513.1-1014 ( $\Delta\theta = 0^\circ.56$ ). False colour count maps at different energies are shown in Figure 3: a point-like object can be easily seen above 3 GeV (central panel), and it appears clearly separated from the much brighter near source and with a brightness comparable to that of the two 3FGL sources close to the North boundary of the image.

The possible counterpart is a rather strong radio source with a spectrum from archive data that is steep up to about 1 GHz and turns to flat at higher frequencies; it is in the CRATES catalogue and in the microwave range it is bright enough to be reported in the Planck catalogue with flux densities at 143 and 217 GHz of  $\sim 200$  mJy. In the POSS images it is at about  $8''$  from a much brighter starlike object ( $R \approx 16$ ) while that corresponding to the radio source is brighter at WISE wavelengths. Photometric data are available in all the four WISE bands and the colours place within the upper part of the blazar locus where are both BL objects and flat spectrum radio quasars. Its blazar nature should be considered safe but an optical spectrum will be useful for establishing the right type.

#### 5.1.23 MST 1546–1002

This flat spectrum radio source is reported in the CRATES and LORCAT catalogues. Its NVSS position corresponds to the fainter object of a pair with a separation of a few arcseconds. These objects appear unresolved in the WISE images and a contamination in the photometric data cannot be excluded. In any case their colours are well placed within the blazar region (blue circle in Figure 1). More data will be useful for understanding their nature and to confirm the association with the  $\gamma$ -ray cluster.

#### 5.1.24 MST 1547–1531

A close pair of objects with similar brightness appear in the SDSS image at the NVSS position of this weak radio source (Figure 2, right panel), one of which (SDSS J154725.68-153237.0) has  $u - r = 0.93$ , while the other

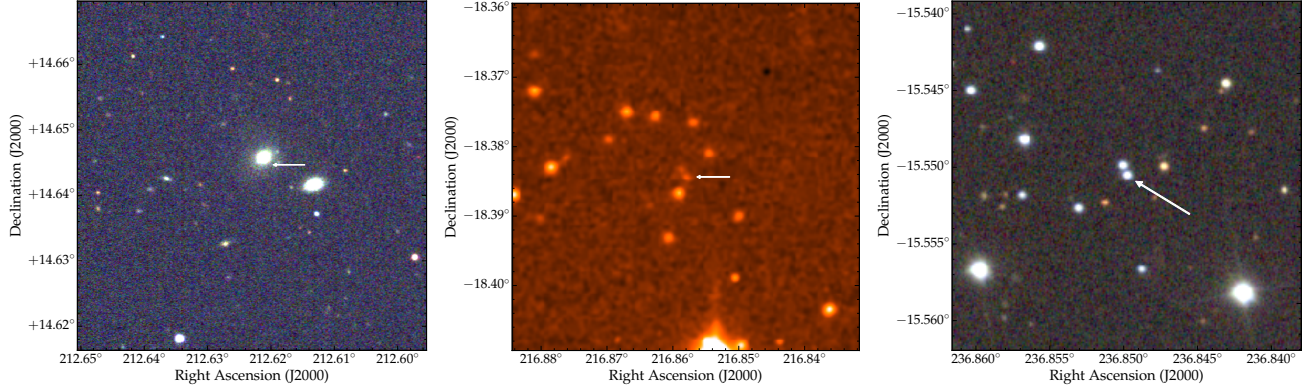


**Fig. 2** *Left panel:* SDSS image (*irg* composite) of the radio galaxy possible counterpart to MST 1410+1438 (see Section 5.1.17), indicated by the horizontal line. The image size is  $200''$ . *Central panel:* SuperCosmos *J*-band field of the radio source close to the centroid of MST 1427–1823 (Section 5.1.18). The image size is  $180''$ . *Right panel:* SDSS image (*irg* composite) of the close pair one of the counterpart to MST 1547–1531 (Section 5.1.24). The image size is  $100''$ . The arrow mark the favorite blazar candidate. For all panels North is in the upper direction and East to the left.

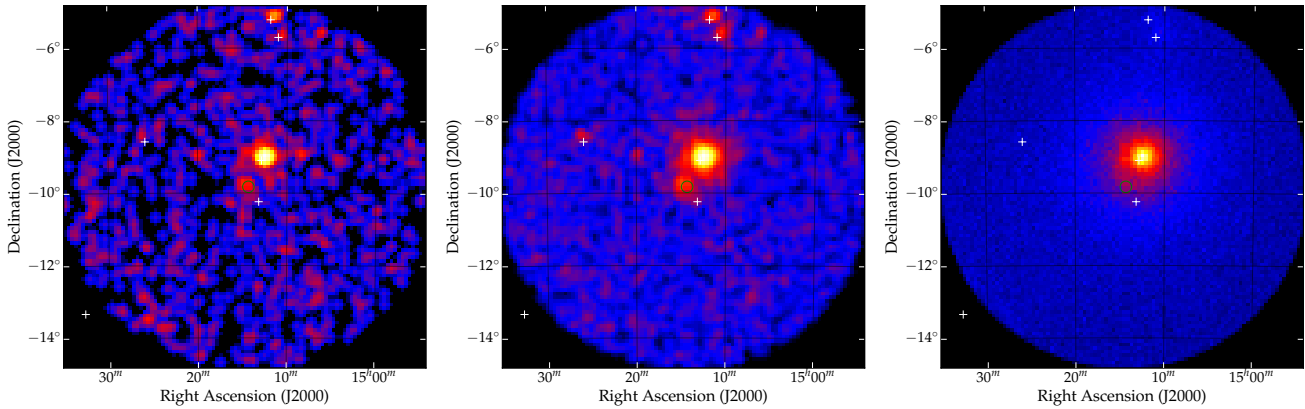


**Fig. 3** False colour count maps in equatorial coordinates at energies higher than 10 GeV (left panel), 3 GeV (central panel), and 100 MeV (right panel), of the sky region centred at the cluster MST 1514–0949 (green circle). The radius of the considered region is  $5^\circ$ . White crosses indicate the positions of 3FGL sources. See Section 5.1.22 for details.

has a redder color index  $u - r = 1.74$ . In the WISE images these two close objects are unresolved and therefore it is not possible to determine their individual colours, but it is interesting that their corresponding point is close to the center of the BL Lac region (open blue square in Figure 1). The bluer object appears as a QSO candidate in Brescia et al. (2015) and should be considered as the primary target for a blazar search.

#### 5.1.25 MST 1605–1142

This source was already reported in the literature as a possible counterpart of a 3EG  $\gamma$ -ray source (Tornikoski et al. 2002; Sowards-Emmerd et al. 2004) and was included in the CGRaBs list (Healey et al. 2008) but it is not present in all the Fermi-LAT catalogues. It is also in the LORCAT catalogue (Massaro et al. 2014)

and in the WIBRaLS samples. No optical spectrum is published. Our finding of a cluster compatible with its position supports the blazar nature of this source.

#### 5.1.26 MST 1640+0640

Very few literature data are available on this radio source. It is reported in the Atlas of Radio/X-ray associations (ARXA, Fleisch 2010) with a high probability of being a QSO. In the two WISE colours plot it lies inside the blazar region.

#### 5.1.27 MST 1643+3317

Five radio sources are in the search radius of this cluster. Two of them, both having a radio flux density of  $\sim 3$  mJy, are “empty field”, i.e. without optical counterpart. The likely optical counterparts of two other

sources, with radio flux densities of  $\sim 10$  and  $20$  mJy, are two similar faint red galaxies, with SDSS photometry of  $r = 20.5$  mag (redshift  $z = 0.608$ ), and  $r = 20.6$  mag (redshift  $z = 0.608$ ). More interesting is the counterpart of the brightest radio source (possibly with two/three components in FIRST) and associated with 1RXS J164339.1+331644, already considered a candidate QSO (Brinkmann et al. 1997; Brescia et al. 2015) In the WISE database only the  $W1 - W2 = 0.44$  colour is available and its nature is not well known because of the lack of an optical spectrum. On the basis of these data no object exhibits clear blazar properties, and the actual counterpart of the  $\gamma$ -ray cluster remain uncertain.

#### 5.1.28 MST 1716+2307

The ML analysis confirmed the existence of a  $\gamma$ -ray source with the high  $\sqrt{TS} = 9.7$ . False colour count maps at different energies are shown in Figure 4: a point-like object can be easily seen above 3 GeV (central and right panel), while it can be confused with the background at energies higher than 100 MeV (left panel). It appears therefore safely established without any possibility of confusion with other sources. There are two weak radio sources within the matching radius and one of them, at the angular distance of  $2'.8$ , has a very red and faint ( $r > 22$ ) SDSS counterpart, while that of the other radio source is a blue object (SDSS J171603.22+230822.8) with a star-like appearance and  $u - r = 0.87$  similar to other  $\gamma$ -ray loud HBL objects (Massaro et al. 2012). It was associated with an X-ray source in the ARXA (Flesch 2010) and reported as QSO candidate by Brescia et al. (2015). No optical spectroscopy is available.

#### 5.1.29 MST 2037–3836

This cluster is located at a longitude close to that of the Galactic Centre in a region with a relatively high background. ML analysis gave for this cluster a significance well below the acceptance threshold ( $\sqrt{TS} = 2.3$ ). MST searches at 8 and 5 GeV extracted a cluster with  $n = 5$  but with magnitude values lower than 20, while at 3 and 20 GeV no cluster was found. The cluster detection is therefore unstable and depends on the considered region. Considering the higher background with respect to other sky regions, the probability that this marginal cluster could be originated by a density fluctuation (the presence of only one photon is critical for its selection) is not negligible. In addition, WISE photometric data of the proposed counterpart are uncertain because it is close to a much brighter star and is poorly resolved in the IR images.

#### 5.1.30 MST 2245–1734

There are three NVSS sources within the searching radius, two of them having a radio flux density of a few mJy without optical counterparts, while the brightest has a faint possible counterpart reported as candidate QSO by Brescia et al. (2015). Its WISE colours are rightly located inside the blazar region. It appears therefore as a good candidate for a HBL object.

## 6 Light curves and variability

Blazars are variable objects and therefore, for the seven clusters for which we derived a flux higher than  $10^{-10}$  photons  $\text{cm}^{-2} \text{s}^{-1}$  in the energy band 3–300 GeV, we extracted light curves by means of standard aperture photometry<sup>4</sup>, with an extraction radius of  $1^\circ$ . For the source MST 1514–0949 (Section 5.1.22), due to the possible contamination from the nearby sources PKS 1510-08 and 3FGL J1513.1-1014, the extraction radius was reduced to  $0^\circ.25$ . Light curves with a 6-months binning and in the 3–300 and 10–300 GeV bands for these clusters are shown in Figures 5 and 6.

For some sources there is a hint of variability, especially in the 3–10 GeV band, on months to years timescales. For example, MST 0137+2247 showed a flux increase around MJD 56600–57000, and for MST 1514–0949 there is evidence of a single, bright flare around MJD 57000. The possibility of contamination from the nearby PKS 1510-08 was excluded by extracting and comparing a light curve for the latter source with a narrow  $0^\circ.5$  radius.

## 7 Summary and discussion

We analysed the first 7 years of *Fermi*-LAT sky at energies higher than 10 GeV by means of the MST algorithm, allowing a robust detection of photon clusters having typical sizes comparable with the instrumental point spread function. In the selection procedure we adopted rather severe threshold values to reduce the possibility of spurious detections due to local background fluctuations.

In the present paper we report 30 new clusters, 26 of them were fully confirmed by the ML analysis that gave  $\sqrt{TS}$  higher than 5; for two clusters we obtained values higher than 4.5, while the remaining two have too low  $TS$  to be considered as confirmed. These clusters

<sup>4</sup>[http://fermi.gsfc.nasa.gov/ssc/data/analysis/scitools/aperture\\_photometry.html](http://fermi.gsfc.nasa.gov/ssc/data/analysis/scitools/aperture_photometry.html)

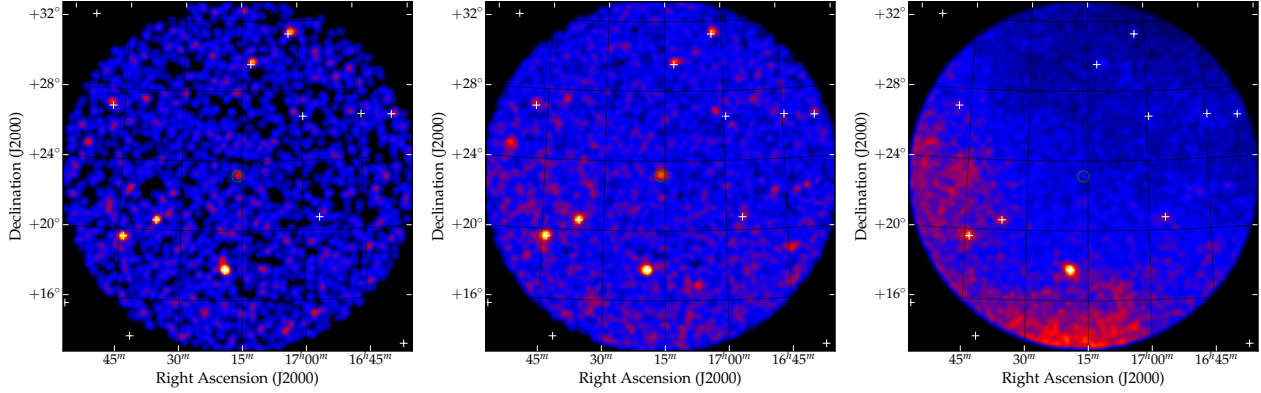


**Fig. 4** False colour count maps in equatorial coordinates at energies higher than 10 GeV (left panel), 3 GeV (center panel) and 100 MeV (right panel) of the sky region centred at the cluster MST J1716+2307 (green circle). The radius of the considered region is  $10^\circ$ . White crosses indicate the positions of 3FGL sources. See Section 5.1.28 for details.

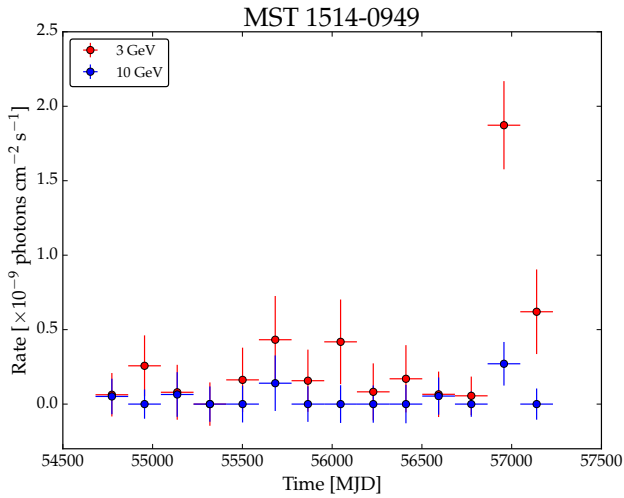


**Fig. 6** Aperture photometry light curves, in the 3–300 and 10–300 GeV bands, extracted with a  $0^\circ.25$  radius around the cluster MST 1514–0949. See text for details.

were also associated with blazar candidates selected on the basis of radio and optical detections. For few of them 6dF and SDSS spectra are available, while some sources appear to be low redshift radio galaxies. The nature of the other sources must be confirmed by new spectroscopic observations.

The blazar nature of our candidates is also supported by their WISE two-colour plot, in which all selected sources are in the blazar region, with a clear dominance for that of BL Lacs. It appears quite unlikely that radio sources, with likely counterparts in the high energy  $\gamma$ -rays, exhibit mid-IR colours typical of BL Lacs and do not belong to this class of AGNs. These researches extend the knowledge on the BL Lac population in two directions: one is towards low brightness sources and the other is concerning the existence of a subclass of

BL Lacs too faint in radio band to be detected in the available surveys. We think that a systematic search for some possible counterparts of  $\gamma$ -ray clusters with  $M$  values lower than the threshold considered here and based on a multifrequency approach, particularly in the mid IR band, could be useful to enrich these studies with new observational results.

Considering the results of Papers I, II, and III, together with those of the present work, to now we have found evidence for 90 blazar or candidate selected for their emission above 10 GeV detected by means of MST cluster search. We remark, however, that these discoveries are due not only to our clustering method but mainly to the improvement of instrumental response functions used for producing the Pass 8 sky and to about double exposure duration with respect to that considered at the epoch of 3FGL catalogue.

We acknowledge use of archival Fermi data. We made large use of the online version of the Roma-BZCAT and of the scientific tools developed at the ASI Science Data Center (ASDC), of the final release of 6dFGS archive, of the Sloan Digital Sky Survey (SDSS) archive, of the NED database and other astronomical catalogues distributed in digital form (VizieR and Simbad) at Centre de Datas astronomiques de Strasbourg (CDS) at the Louis Pasteur University.

## References

- Ackermann, M., Ajello, M., Allafort, A., Asano, K., Atwood, W.B., Baldini, L., Ballet, J., Barbiellini, G., *et al.*: *Astrophys. J.* **765**, 54 (2013)
- Ackermann, M., Ajello, M., Asano, K., Atwood, W.B., Axelsson, M., Baldini, L., Ballet, J., Barbiellini, G., *et al.*: *Science* **343**, 42 (2014)

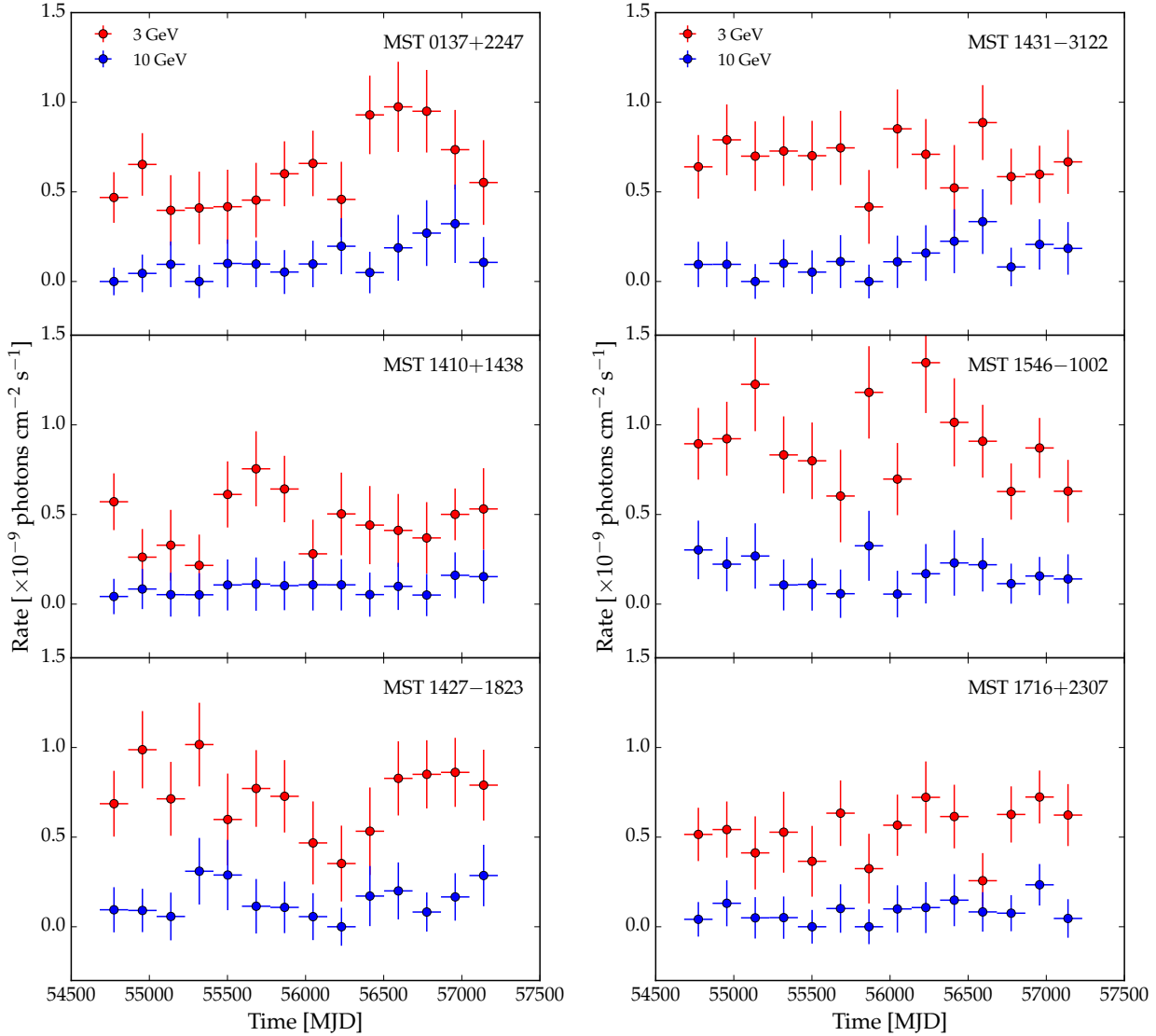


**Fig. 5** Aperture photometry light curves, in the 3–300 and 10–300 GeV bands, extracted with a  $1^\circ$  radius around the clusters MST 0137+2247, MST 1410+1438, MST 1427–1823, MST 1431–3122, MST 1546–1002 and MST 1716+2307. See text for details.

Alam, S., Albareti, F.D., Allende Prieto, C., Anders, F., Anderson, S.F., Anderton, T., Andrews, B.H., Armengaud, E., Aubourg, É., Bailey, S., et al.: *Astrophys. J. Suppl. Ser.* **219**, 12 (2015)

Appenzeller, I., Thiering, I., Zickgraf, F.-J., Krautter, J., Voges, W., Chavarria, C., Kneer, R., Mujica, R., Pakull, M., Rosso, C., Ruzicka, F., Serrano, A., Ziegler, B.: *Astrophys. J. Suppl. Ser.* **117**, 319 (1998)

Arsioli, B., Fraga, B., Giommi, P., Padovani, P., Marrese, P.M.: *Astron. Astrophys.* **579**, 34 (2015)

Brescia, M., Cavuoti, S., Longo, G.: *Mon. Not. R. Astron. Soc.* **450**, 3893 (2015)

Brinkmann, W., Siebert, J., Feigelson, E.D., Kollgaard, R.L., Laurent-Muehleisen, S.A., Reich, W., Fuerst, E., Reich, P., Voges, W., Truemper, J., McMahon, R.: *Astron. Astrophys.* **323**, 739 (1997)

Campana, R., Massaro, E., Bernieri, E.: *Astrophys. Space Sci.* **361**, 185 (2016a)

Campana, R., Massaro, E., Bernieri, E.: *Astrophys. Space Sci.* **361**, 183 (2016b)

Campana, R., Massaro, E., Gasparrini, D., Cutini, S., Tramacere, A.: *Mon. Not. R. Astron. Soc.* **383**, 1166 (2008)

Campana, R., Bernieri, E., Massaro, E., Tinebra, F., Tosti, G.: *Astrophys. Space Sci.* **347**, 169 (2013)

Campana, R., Massaro, E., Bernieri, E., D’Amato, Q.: *Astrophys. Space Sci.* **360**, 19 (2015)

Condon, J.J., Cotton, W.D., Greisen, E.W., Yin, Q.F., Perley, R.A., Taylor, G.B., Broderick, J.J.: *Astron. J.* **115**, 1693 (1998)

Cutri, R.M., Wright, E.L., Conrow, T., Fowler, J.W., Eisenhardt, P.R.M., Grillmair, C., Kirkpatrick, J.D., Masci, F., et al.: Explanatory Supplement to the AllWISE Data Release Products. Technical report, (November 2013)

- D'Abrusco, R., Longo, G., Walton, N.A.: *Mon. Not. R. Astron. Soc.* **396**, 223 (2009)
- D'Abrusco, R., Massaro, F., Ajello, M., Grindlay, J.E., Smith, H.A., Tosti, G.: *Astrophys. J.* **748**, 68 (2012)
- D'Abrusco, R., Massaro, F., Paggi, A., Smith, H.A., Masetti, N., Landoni, M., Tosti, G.: *Astrophys. J. Suppl. Ser.* **215**, 14 (2014)
- Evans, P.A., Osborne, J.P., Beardmore, A.P., Page, K.L., Willingale, R., Mountford, C.J., Pagani, C., Burrows, D.N., Kennea, J.A., Perri, M., Tagliaferri, G., Gehrels, N.: *Astrophys. J. Suppl. Ser.* **210**, 8 (2014)
- Flesch, E.: *Proc. Astron. Soc. Aust.* **27**, 283 (2010)
- Gregory, P.C., Vavasour, J.D., Scott, W.K., Condon, J.J.: *Astrophys. J. Suppl. Ser.* **90**, 173 (1994)
- Hartman, R.C., Bertsch, D.L., Bloom, S.D., Chen, A.W., Deines-Jones, P., Esposito, J.A., Fichtel, C.E., Friedlander, D.P., Hunter, S.D., McDonald, L.M., Sreekumar, P., Thompson, D.J., Jones, B.B., Lin, Y.C., Michelson, P.F., Nolan, P.L., Tompkins, W.F., Kanbach, G., Mayer-Hasselwander, H.A., Mücke, A., Pohl, M., Reimer, O., Kniffen, D.A., Schneid, E.J., von Montigny, C., Mukherjee, R., Dingus, B.L.: *Astrophys. J. Suppl. Ser.* **123**, 79 (1999)
- Healey, S.E., Romani, R.W., Cotter, G., Michelson, P.F., Schlafly, E.F., Readhead, A.C.S., Giommi, P., Chaty, S., Grenier, I.A., Weintraub, L.C.: *Astrophys. J. Suppl. Ser.* **175**, 97 (2008)
- Jones, D.H., Saunders, W., Colless, M., Read, M.A., Parker, Q.A., Watson, F.G., Campbell, L.A., Burkey, D., *et al.*: *Mon. Not. R. Astron. Soc.* **355**, 747 (2004)
- Jones, D.H., Read, M.A., Saunders, W., Colless, M., Jarrett, T., Parker, Q.A., Fairall, A.P., Mauch, T., *et al.*: *Mon. Not. R. Astron. Soc.* **399**, 683 (2009)
- Mahony, E.K., Croom, S.M., Boyle, B.J., Edge, A.C., Mauch, T., Sadler, E.M.: *Mon. Not. R. Astron. Soc.* **401**, 1151 (2010)
- Maselli, A., Melandri, A., Nava, L., Mundell, C.G., Kawai, N., Campana, S., Covino, S., Cummings, J.R., *et al.*: *Science* **343**, 48 (2014)
- Massaro, E., Nesci, R., Piranomonte, S.: *Mon. Not. R. Astron. Soc.* **422**, 2322 (2012)
- Massaro, E., Maselli, A., Leto, C., *et al.*: *Multifrequency Catalogue of Blazars*, 5th edn. Aracne Editrice, Rome (2014)
- Massaro, F., D'Abrusco, R.: *Astrophys. J.* **827**, 67 (2016). doi:10.3847/0004-637X/827/1/67
- Massaro, F., Thompson, D.J., Ferrara, E.C.: *Astron. Astrophys. Rev.* **24**, 2 (2016)
- Massaro, F., D'Abrusco, R., Ajello, M., Grindlay, J.E., Smith, H.A.: *Astrophys. J. Lett.* **740**, 48 (2011)
- Massaro, F., Paggi, A., Errando, M., D'Abrusco, R., Masetti, N., Tosti, G., Funk, S.: *Astrophys. J. Suppl. Ser.* **207**, 16 (2013)
- Mauch, T., Murphy, T., Buttery, H.J., Curran, J., Hunstead, R.W., Piestrzynski, B., Robertson, J.G., Sadler, E.M.: *Mon. Not. R. Astron. Soc.* **342**, 1117 (2003)
- Mickaelian, A.M., Hovhannisyan, L.R., Engels, D., Hagen, H.-J., Voges, W.: *Astron. Astrophys.* **449**, 425 (2006)
- Padovani, P., Giommi, P.: *Mon. Not. R. Astron. Soc.* **277**, 1477 (1995)
- Schwope, A., Hasinger, G., Lehmann, I., Schwarz, R., Brunner, H., Neizvestny, S., Ugryumov, A., Balega, Y., Trümper, J., Voges, W.: *Astronomische Nachrichten* **321**, 1 (2000)
- Smart, R.L., Nicastro, L.: *VizieR Online Data Catalog* **1324** (2013)
- Sowards-Emmerd, D., Romani, R.W., Michelson, P.F., Ulvestad, J.S.: *Astrophys. J.* **609**, 564 (2004)
- The Fermi-LAT Collaboration: *ArXiv e-prints* (2015). 1508.04449
- Titov, O., Stanford, L.M., Johnston, H.M., Pursimo, T., Hunstead, R.W., Jauncey, D.L., Maslennikov, K., Boldycheva, A.: *Astron. J.* **146**, 10 (2013). doi:10.1088/0004-6256/146/1/10
- Tornikoski, M., Lähteenmäki, A., Lainela, M., Valtaoja, E.: *Astrophys. J.* **579**, 136 (2002)
- Voges, W., Aschenbach, B., Boller, T., Bräuninger, H., Briel, U., Burkert, W., Dennerl, K., Englhauser, J., Gruber, R., Haberl, F., Hartner, G., Hasinger, G., Kürster, M., Pfeffermann, E., Pietsch, W., Predehl, P., Rosso, C., Schmitt, J.H.M.M., Trümper, J., Zimmermann, H.U.: *Astron. Astrophys.* **349**, 389 (1999)
- White, R.L., Becker, R.H., Helfand, D.J., Gregg, M.D.: *Astrophys. J.* **475**, 479 (1997)
- Wright, E.L., Eisenhardt, P.R.M., Mainzer, A.K., Ressler, M.E., Cutri, R.M., Jarrett, T., Kirkpatrick, J.D., Padgett, D., *et al.*: *Astron. J.* **140**, 1868 (2010)